



Project 070 Reduction of nvPM Emissions from Aero-Engine Fuel Injectors

Georgia Institute of Technology

Project Lead Investigator

Wenting Sun
Associate Professor
School of Aerospace Engineering
Georgia Institute of Technology
270 Ferst Drive, Atlanta, GA 30332
404-894-0524
wenting.sun@aerospace.gatech.edu

University Participants

Georgia Institute of Technology (Georgia Tech)

- P.I.: Dr. Wenting Sun
- FAA Award Number: 13-C-AJFE-GIT-080
- Period of Performance: September 01, 2023, to September 30, 2024
- Task:
 1. Spray characterization and measurement of non-volatile particulate matter formation

Project Funding Level

The total amount of funding from the Federal Aviation Administration (FAA) is \$1,500,000. The funding match includes \$1,350,000 from the Georgia Institute of Technology and \$150,000 from Honeywell.®

Investigation Team

Georgia Institute of Technology

Wenting Sun, (P.I.), Task 1,3
Adam Steinberg, (co-P.I.), Task 1
Ellen Yi Chen, (co-P.I.), Task 1
Shawn Wehe, (research engineer), Task 1,3
Rahul Vishwanath, (postdoctoral fellow), Task 1,3
Dominic Olimid, (graduate student), Task 1
Eric Douglas, (graduate student), Task 1
Adhav Arulanandan, (graduate student), Task 1
Andrew Fan, (graduate student), Task 1

Honeywell. Inc

Rudy Dudebout, (co-P.I.), Task 2
Fang Xu, (co-P.I.), Task 2

Project Overview

Reducing non-volatile particulate matter (nvPM) from gas turbine engines is essential for improving air quality and decreasing the environmental impact of aviation. However, predicting and controlling nvPM remains a challenge because of the complicated physical and chemical processes at play. The proposed research will characterize the fuel spray and nvPM

® Honeywell is a registered trademark of Honeywell International, Inc., Charlotte, North Carolina.





formation for optimizing the design of an aeronautical gas turbine fuel injector to reduce nvPM at flight-relevant conditions. In this project, the ASCENT Project 070 team developed a sector combustor containing three fuel injectors. The sector combustor is a generic rich-quench-lean (RQL) jet engine combustor equipped with the actual fuel injectors used in Honeywell's auxiliary power unit (APU). The combustor was fabricated through three-dimensional (3-D) printing, and the fuel injectors are directly provided by Honeywell. The combustor and high-pressure system were detailed in a previous report and are presented briefly in the next section. The research focus of this year is on conducting an experimental campaign to characterize droplet size and measure nvPM volume fraction distribution in the primary zone of the combustor, a region between the fuel injector and downstream quenching holes. The performance of combustion in this rich region dictates the overall performance of the combustor therefore it is the research focus of this project.

Task 1 – Spray Characterization and Measurement of Non-volatile Particulate Matter Formation

Georgia Institute of Technology

Objective

The objective of Task 1 is to obtain drop-size distribution for spray injectors using phase doppler particle anemometry (PDPA) and to quantify the nvPM volume fraction by laser-induced incandescence (LII) under a broad range of conditions for Jet A fuel and sustainable aviation fuel (SAF), respectively.

Research Approach

In this year, droplet-size distributions are obtained to characterize liquid fuel spray using PDPA at different pressure, inlet temperature, and equivalence ratio conditions in both reacting and non-reacting conditions. **This is the first such measurement performed in a three-sector combustor housed in a pressure vessel due to its unconventional configuration.** Additionally, quantitative measurements of soot volume fraction have been obtained using two-color LII at different operating conditions. Both these measurements are performed using Jet A fuel and SAF to compare the combustion characteristics of both the fuels and their blends. The SAF employed in this study is the hydroprocessed esters and fatty acids (HEFA) from World Energy. Results are presented below in corresponding sections.

Subtask 1.1: Droplet-size measurement using PDPA

PDPA utilizes the light scattering interferometry technique wherein interference signals are created by two intersecting laser beams in a small measurement volume of interest. As individual particles/droplets move through this volume, a shift in the frequency of scattered light is detected which is proportional to the particle velocity. Additionally, there is a phase shift in the detected interference signal which is proportional to the size of the particle. Hence, simultaneous information on particle velocity and size can be obtained with high spatial and temporal accuracy using this technique. One of the major advantages of PDPA is that the fringe patterns produced by the particles are obtained only from the scattered light signals produced within the probe volume, which eliminates signal interference from other sources. For environments with high spatial and temporal variations in density, the technique suffers from beam steering, which gives rise to low signal to noise ratios.

For measuring droplet sizes, PDPA requires off-axis scattering angles in the range of 30-70 degrees. This presents a challenge for confined combustors housed in pressure vessels wherein such scattering angles are not available. To overcome this difficulty, a creative mirror system has been proposed and mounted inside the pressure vessel to obtain scattering angles up to 40 degrees in the plane of measurement.

The PDPA system (from Dantec Dynamics®) consists of a diode-pumped solid state (DPSS) laser transmitter capable of emitting a pair of 1000 mW, 561 nm laser beams, with each beam frequency shifted by 40 MHz using a Bragg cell. Although the system can operate with two pairs of laser beams at 532 nm and 561 nm, only one pair is utilized for droplet-size measurements. The laser beam pair is then sent into a transmitter probe (TSI, Inc.) through fiber optic cables, where a lens having a focal length of 61 cm is used to focus the two beams into the sample measurement volume. The phase-shifted light scattered from the droplet in the small measurement volume is then collected by a receiver module through two mirrors placed and aligned such that the collection angle of the scattered light is approximately 40 degrees. The collected light passes through a three slit mask mounted onto the receiver, where the light through each of the slits is

® Dantec Dynamics is a registered trademark of Dantec Dynamic, Inc., Mahwah, New Jersey.



focused separately and transmitted through fiber optical cables into the basic spectrum analyzer (BSA). The analyzer is capable of measuring signal bursts at frequencies up to 400 kHz and subsequently produce instantaneous drop-size distributions.

The combustor wall (liner) includes three Honeywell aircraft swirl injectors on the dome face, representing typical multiple sectors of an aeroengine combustor, as illustrated in Figure 1b. The combustion liner has four fused quartz windows for optical access. Two windows on opposing sides enable laser access across all three injectors, and two windows on top provide visual access to the rich-burn and lean-burn regions. The mirror system is mounted onto the inner face of the quartz vessel window flange as shown in Figure 1a. It consists of two mirrors, with the first mirror having a 7.5 cm diameter clear aperture and the second mirror having a 15 x 10 cm rectangular area. They are aligned together to collect the scattered light from the droplets and focus onto the PDPA receiver module. The entire mirror system mount is made of stainless steel to minimize material deformation from high temperature air flowing through the vessel. The measurement region was restricted to a 5 cm x 5 cm area on left-hand side of the central nozzle as shown in Figure 1a, due to the constraints on the current PDPA and mirror system.

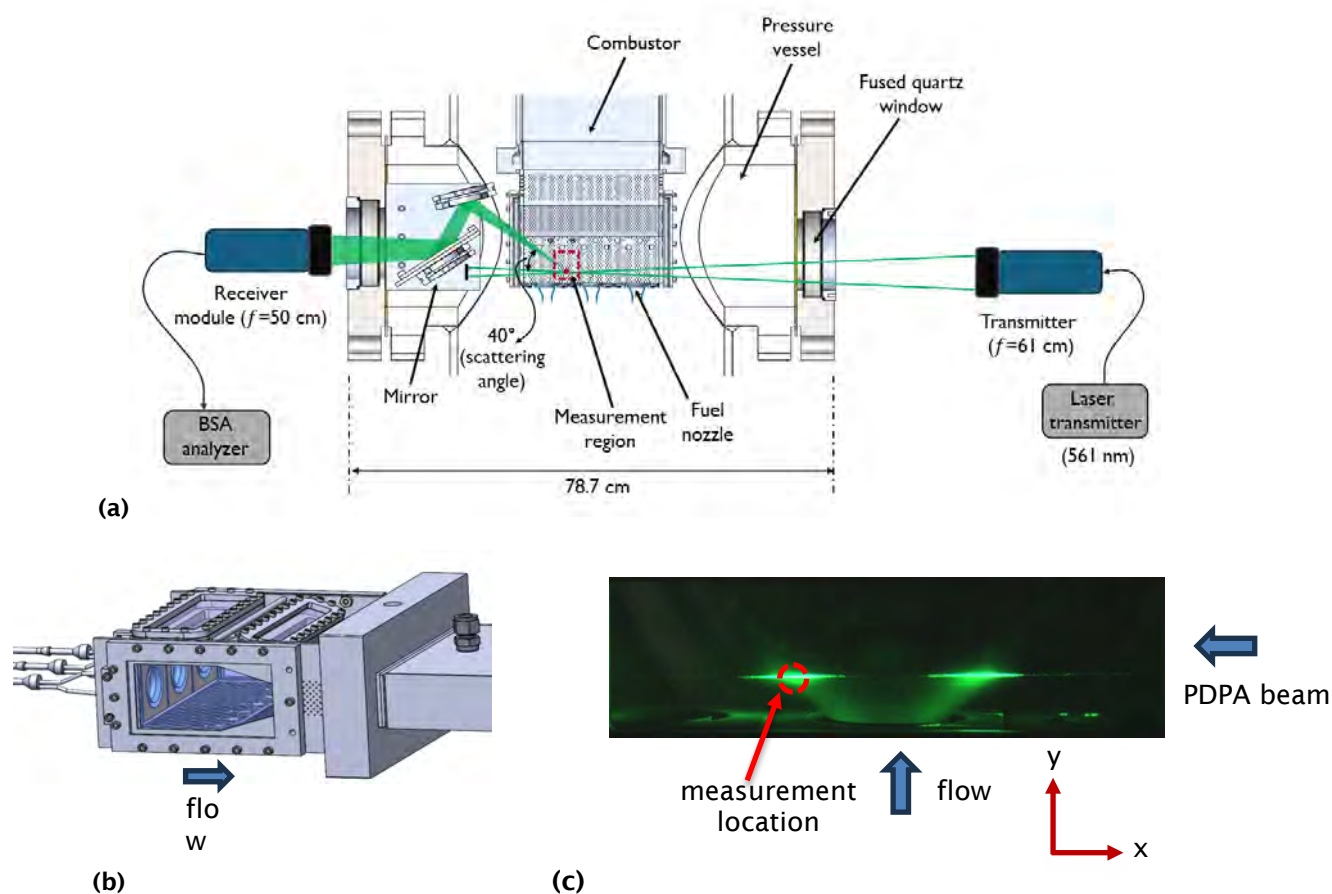


Figure 1. (a) Schematic of the PDPA setup showing the two-mirror configuration to obtain required scattering angles in a confined vessel for the depicted measurement region. (b) View of the combustor depicting the three fuel nozzles and quartz windows for optical access. (c) Raw image of Mie scattering from the central injector spray along with the PDPA laser beam oriented in the vertical plane (perpendicular to the flow direction) passing through the spray. PDPA: phase doppler particle anemometry, BSA: basic spectrum analyzer.

Experiments are performed at both cold flow and reacting flow conditions to study the effect of combustion environment on droplet vaporization and subsequent drop-size. In all cases, only the central injector is operated so that the droplets do



not cover the combustor windows which will affect PDPA measurements, especially in cold-flow conditions. A total of four operating conditions were chosen with varying pressure (0 psig, 35.3 psig, 85.3 psig), preheat temperature (450 K, 600 K), and global equivalence ratio (0.264, 0.315) for both Jet A fuel and SAF. It is to be noted that since the combustor is run on a RQL concept, the local equivalence ratios in the rich-burn region immediately downstream of the nozzles may vary from 1.22 to 1.45, depending on the global equivalence ratio. Although only the central injector is utilized while operating the combustor for PDPA measurements, the local equivalence ratio for that injector should remain the same. For cold flow conditions, ten measurement locations were chosen, whereas for reacting conditions only four locations were chosen where minimal soot was present just downstream of the nozzle dump plane along the spray cone.

At every spatial location, a total of 10,000 instantaneous measurements were made for all cases. But in certain conditions where the signal to noise ratio was slightly poor, the total measurement counts reduced. Nonetheless, the frequency distributions were repeatable for all conditions. The current fuel injectors utilized in this study are pre-filming air blast-type assisted with surrounding swirl air for jet breakup. Figure 2 shows the number frequency and Sauter mean diameter (SMD) distribution at various spatial locations for a non-reacting Jet A fuel spray at 35.3 psig pressure and 450 K preheat temperature. Zero on the x-axis represents the center axis of the center fuel injector. The Y axis represents the distance from the combustor dome face. The droplet diameters are typically in a broad range of 1-100 μm at most locations, although the maximum frequencies are within the small range of 10-40 μm suggesting good atomization at these operating conditions. Due to the right skewed nature of the number frequency distributions, the SMD values tend to shift towards larger diameters, but the peak diameters are always lower.

It can be seen from the results shown in Figure 2, the SMD values of the droplets reduced with increasing axial distance downstream of the injector along the spray cone as the swirling air assists in secondary atomization of the spray. Another reason for the decrease of SMD along the flow direction is vaporization of the droplets while flowing downstream. It is to be noted that the present PDPA system can detect droplets only in the range of 0.1-170 μm based on the slit size and mask used on the receiver module. As seen from the frequency distributions, this range was sufficient to cover the entire spray as the probability of detecting droplets larger than 150 μm was almost negligible.

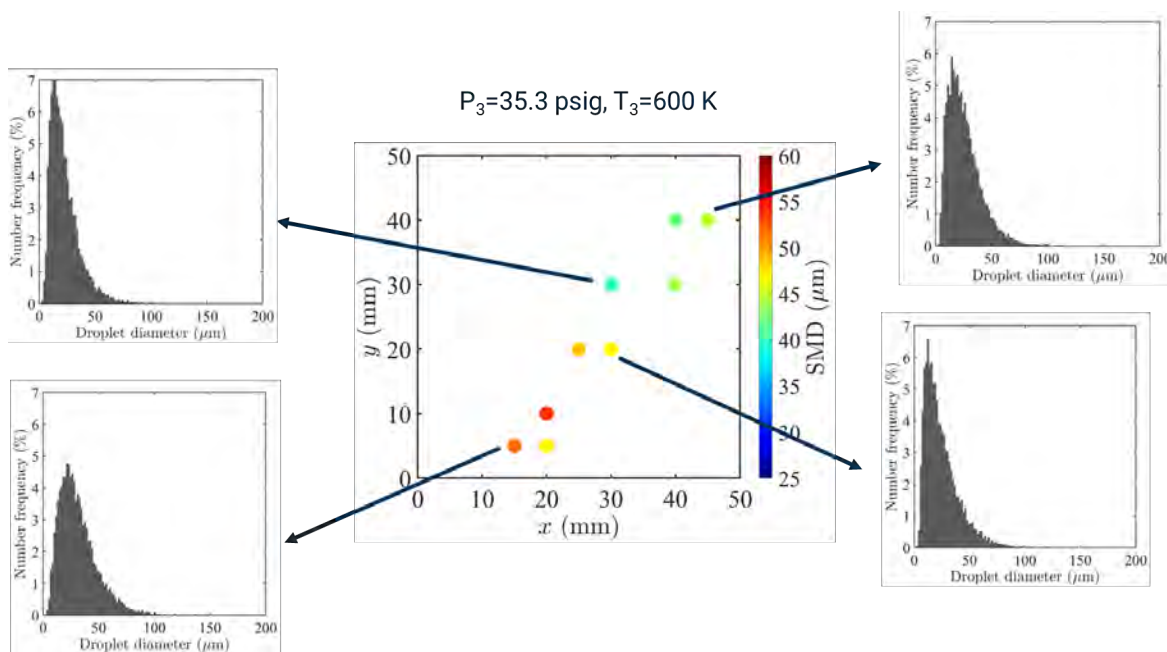


Figure 2. Sauter mean diameters (SMDs) and number frequency distributions from PDPA measurements for non-reacting Jet A fuel spray at 35.3 psig pressure and 450 K preheat temperature.

Figure 3 shows the SMD values measured at different operating conditions for Jet A in non-reacting spray. Apart from the general trend of decreasing diameters with increasing downstream distance, there are trends observed with different



pressures and preheat temperatures. With increasing operating pressure, the SMD decreases for a given location and preheat temperature. This is due to the increase in Reynolds number of the surrounding air causing larger relative velocities between the liquid and gas phase, thereby inducing faster primary breakup of liquid jet and subsequent smaller droplets. The amount of reduction is highly dependent on the Reynolds number range or the operating pressure. The reduction in SMD due to increasing preheat for surrounding air is due to droplets being able to evaporate faster as they travel downstream of the fuel nozzle. Compared to the atmospheric conditions, the mean SMD values have decreased by more than two times when the combustor is operated at 85.3 psig pressure at a preheat of 600 K. Our results suggest that measurements and characterization need to be conducted in practical engine operating conditions.

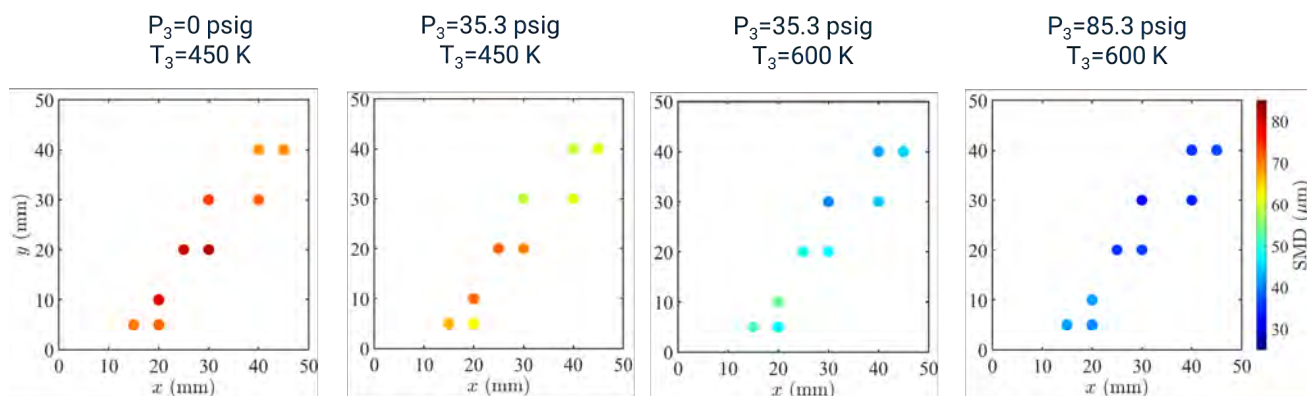


Figure 3. Spatial variation of Sauter mean diameter (SMD) values for non-reacting Jet A fuel spray at different operating conditions.

To study the effect of reacting conditions on the spray, measurements were performed with the same PDPA configuration at the same operating conditions. It is to be noted that the current combustor operates liquid spray flames that produce large amounts of soot, especially in the primary zone of the combustor. Since the soot particles are mostly in solid phase at the measurement region, they can be detected as particles by the device which corrupts the actual droplet signals. To avoid this, the measurement region is confined to a small region 10-20 mm downstream of the dump plane within the spray cone. This region is largely devoid of soot, apart from small fluctuations in the flame where soot/flame can be entrained into these regions. Four measurements points (matching the non-reacting conditions) were possible for all the reacting conditions. The number frequency distributions for non-reacting and reacting conditions are compared in Figure 4 for Jet A fuel at 35.3 psig pressure and 600 K preheat at two different locations. For the reacting case, the distributions seem to shift towards larger diameters for all locations. This is counter-intuitive in the sense that reaction/flame should help the droplets evaporate faster adding to the preheat leading to smaller droplets. The plots in Figure 4 suggests that the smaller droplets not only evaporate faster but are almost non-existent, leaving only the larger droplets being detected. Hence, it is very possible that the SMD values are considerably higher in the reacting cases as compared to the non-reacting cases owing to the disappearance of small droplets which are vaporized promptly. An increase in almost 15-20 μm is observed for SMD in reacting cases compared to their non-reacting counterparts. This change was consistently observed for all cases at the same spatial location and operating conditions. Additionally, these distribution changes also provide information on the number of smaller diameter droplets available in reacting cases at any downstream location. If it were a non-sooting flame, reliable measurements (uncorrupted from the presence of soot) would be possible in the entire flame region providing a good insight on droplet evaporation and breakup for comparison between non-reacting and reacting conditions. It is worth mentioning that the signal to noise ratio was much lower in reacting cases at the same measurement location due to laser extinction as the laser beam passes through the flame/spray regions from the side nozzles before reaching the measurement zone. Additionally, the large density differences within the flow leads to beam steering causing the PDPA focal region to keep shifting, in turn reducing the signal rate.

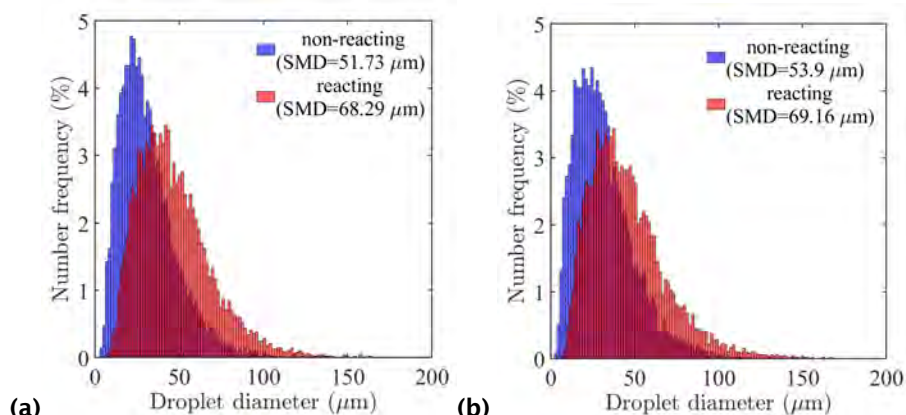


Figure 4. Comparison of number frequency distributions for Jet A fuel at reacting and non-reacting conditions with 35.3 psig pressure and 600 K preheat temperature for locations (a) $x=15$ mm, $y=5$ mm (b) $x=20$ mm, $y=10$ mm.

The second part of the measurements involved utilizing SAF for the measurements at the same conditions as Jet A fuel. The SAF used here is a HEFA-based fuel with almost negligible amount of aromatic content in it. Figure 5 shows the comparison in number frequency distributions between Jet A fuel and SAF in the non-reacting case for the same operating conditions. It is seen that the SAF spray produces slightly smaller droplets compared to Jet A fuel spray, giving a smaller SMD value. This is mostly due to the changes in physical properties of the two different fuels. The SAF utilized in this study has ~10% lower surface tension as compared to Jet A fuel. Reduction in surface tension helps in formation of new surface areas promoting droplet/jet breakup, thereby creating smaller droplets. This can also be looked at in terms of Weber number which is inversely proportional to the surface tension force. The higher the Weber number, better is the atomization quality of the liquid spray. Also, at temperatures above 100° C, the vapor pressure of SAF is ~5% higher than Jet A fuel which can contribute to better vaporization and smaller droplets. The variation in SMD values at different operating conditions followed similar trends as Jet A fuel at all the measurement locations. Similar trends were observed for reacting cases between Jet A fuel and SAF as shown in Figure 6. The frequency distributions for SAF case shifted towards smaller diameters, suggesting an overall reduction in SMD for a given condition and location.

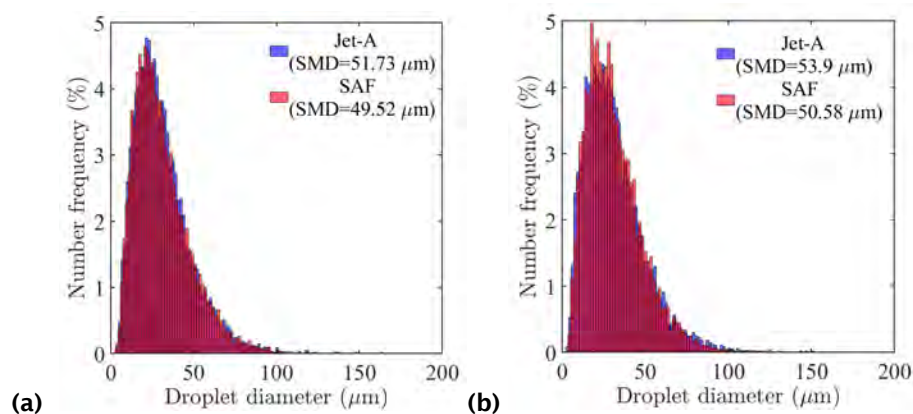


Figure 5. Comparison of number frequency distributions for Jet A fuel and SAF at non-reacting conditions with 35.3 psig pressure and 600 K preheat temperature for locations (a) $x=15$ mm, $y=5$ mm (b) $x=20$ mm, $y=10$ mm.

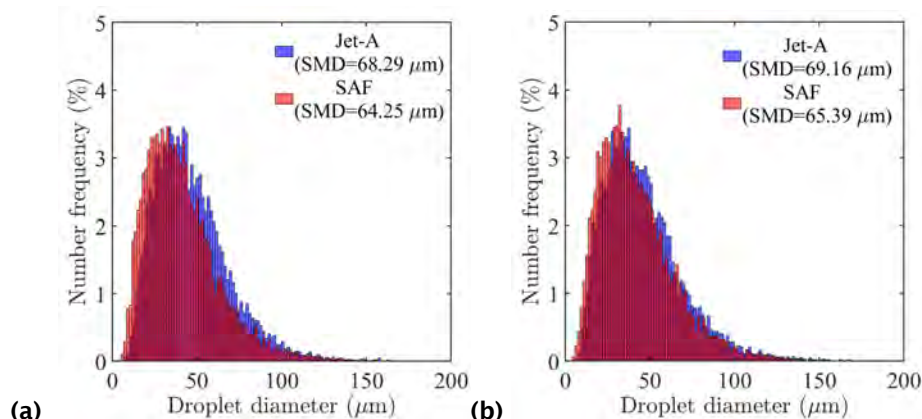


Figure 6. Comparison of number frequency distributions for Jet A fuel and SAF at reacting conditions with 35.3 psig pressure and 600 K preheat temperature for locations (a) $x=15$ mm, $y=5$ mm (b) $x=20$ mm, $y=10$ mm.

Since the availability of SAF is limited at the current scenario due to production/supply issues, blending sustainable fuels with neat Jet A fuel is considered a viable option. Due to small changes in physical and chemical properties of these blended fuels as compared to their neat counterparts, their spray and combustion characteristics are still not well known. Hence, measurements were also performed at the same locations by blending the neat fuels in a 50-50% by volume (further referred to as 50-50 blend). Figure 7 shows the SMD comparison between the neat fuels and their blend for 35.3 psig pressure and 600 K preheat. From the previous discussions, it was seen that SAF generally produced slightly smaller droplets. Interestingly, the 50-50 blend does not show a very clear trend for a given operating condition. As seen from the SMD comparison, the 50-50 blend produced slightly larger SMDs compared to their neat fuels closer to the nozzle. But for locations more downstream ($y > 20$ mm), the SMD values were comparable to neat Jet A fuel. In the present study, physical properties such as surface tension, viscosity and density for the 50-50 blend generally lie in between their neat fuel properties. Hence, their behavior in spray breakup and atomization is expected to occur in the same trend. But the results show that the atomization behavior can change significantly with location (which can be a proxy for time) and/or operating conditions. While PDPA can measure the SMD, it cannot measure the absolute number of droplets. However, the SMD is controlled by the existing droplets regardless of their absolute number. Therefore, there exists a possibility that at more downstream locations, SAF component in the blend might evaporate faster and hence, most droplets in the measurement region are from Jet A fuel, thus the droplet size (SMD) is dominated by Jet A fuel. Therefore, it is closer to the results of Jet A fuel even the 50-50 blend. In fact, the vapor pressure of the blend in the current study is slightly lower compared to their neat fuels. So, this might affect the droplet size based on the location within the spray. Further investigations are necessary to draw firm conclusions on understanding the atomization behavior of blended fuels, which will be conducted in future testing.

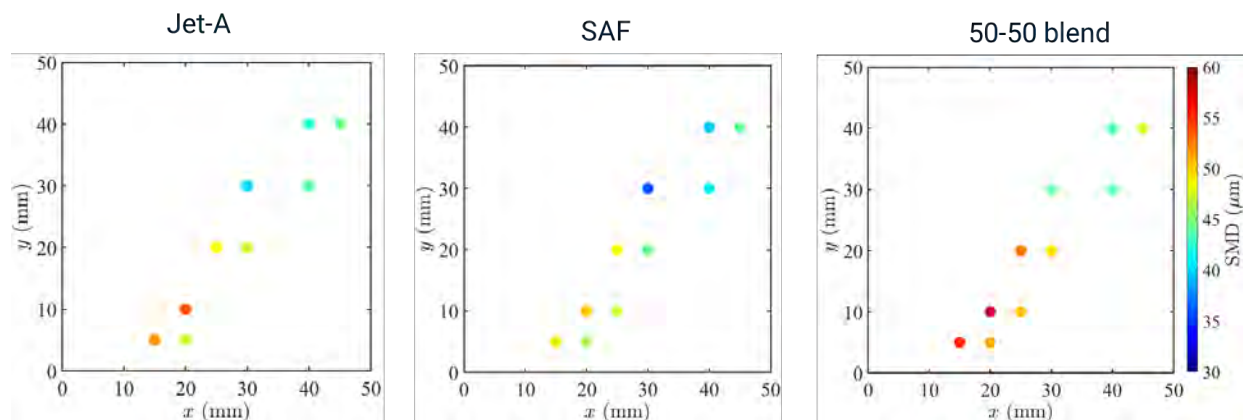


Figure 7. Spatial variation of Sauter mean diameter (SMD) values for non-reacting spray with neat Jet A, neat SAF and 50-50 blend at operating conditions of 35.3 psig pressure and 600 K preheat temperature.

Subtask 1.2: Two-color LII for nvPM/soot measurements

LII involves heating soot particles using a short pulsed high-energy laser instantaneously. When the particles absorb this energy, they re-emit through radiation in a broadband wavelength spectrum governed by Planck's law. This resulting magnitude of the incandescence signal just after the laser pulse absorption can be correlated with the particle volume fraction, whereas the signal decay rate profile is dependent on the primary particle size in the detection region. To quantify the volume fraction, the incandescence signal must be calibrated with a known value of soot concentration in a standard burner using a different detection technique. This can also be done using an in-situ extinction technique in the same flame simultaneously with LII. But these methods incur high uncertainties in the calibration, mainly due to unknown soot optical properties. In this study, a calibration lamp of known radiance-wavelength relationship is utilized where the camera intensity can be calibrated. The main advantage of this method relies upon the fact that the quantification is completely independent of the flame conditions, type of fuel and the optical setup. In fact, any errors that might occur due to the parameters within the optical setup is auto compensated even though the errors due to unknown soot optical properties still exist.

The schematic of the LII setup used in the current study is shown in Figure 8a. The soot particles are heated using a ~2 J/pulse Nd:YAG laser (Quanta-ray® Pro-250) emitting a 1064 nm beam having a pulse width of 8-12 ns. The infrared wavelength of 1064 nm helps in avoiding interference due to laser induced fluorescence occurring from polycyclic aromatic hydrocarbons either present inherently in the fuel or formed after combustion. The gaussian laser beam is then shaped into a collimated sheet of nearly top hat profile using a three-lens combination, consisting of a cylindrical concave lens ($f=-25.4$ mm) and two cylindrical convex lenses ($f=400$ mm and $f=1000$ mm). After the first lens, the diverging sheet was passed through an iris to obtain only the central part of the gaussian profile before hitting the second lens. Another iris restricted the final collimated sheet height to about 27 mm with a beam waist of <1 mm at the combustor centerline. The laser energy was controlled to obtain a fluence of around 0.3-0.4 J/cm² throughout the sheet height, to operate within the low-fluence LII regime where the incandescence signal is nearly independent of the fluctuations in laser energy. The broadband incandescence signal emitted by the soot particles after laser absorption is captured using an intensified charge coupled device (CCD) camera (PI-MAX® 4) after passing through an image splitter. The image splitter (LaVision®) consists of a splitting prism which separates the same imaging area to be viewed at two different wavelengths filtered at 447±60 nm and 680±42 nm. This helps in obtaining soot temperature through two color incandescence detection instantaneously throughout the imaging region. The camera intensities at both the wavelengths are calibrated using the known radiance from a calibration lamp mounted inside an integrating sphere (Sphere Optics®), see Figure 8b. The light source is kept at the same location as the laser sheet with the exact detection setup and settings as the LII images. The LII signal was captured with an exposure time of 80 ns after the peak laser absorption with the camera and the laser being

® Quanta-ray is a registered trademark of Newport Corporation, Santa Clara, California.

® Pi-Max is a registered trademark of Teledyne Digital Imaging US, Inc., Thousand Oaks, California.

® LaVision is a registered trademark of LaVision GmbH, Gottingen, Germany.

® Sphere Optics is a registered trademark of SphereOptics GmbH, Herrsching, Germany.



timed using a delay generator. The images were flat-field corrected for spatial intensity variation through the imaging path and camera response. A total of 500 images were captured for each experimental condition to obtain mean soot volume fraction distributions.

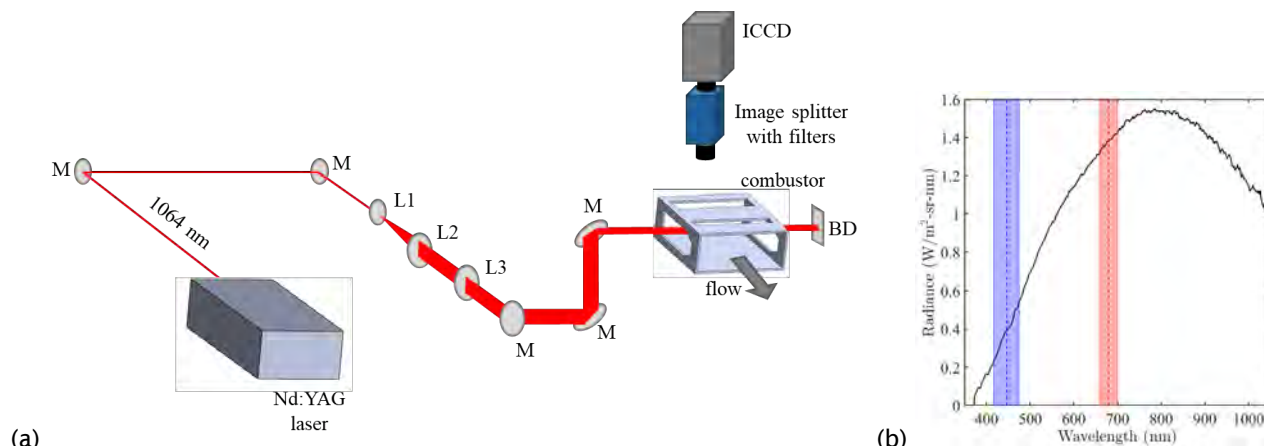


Figure 8. (a) Schematic of the two-color LII setup. The image splitter splits the image and passes through two filters centered at 447 nm and 680 nm onto the ICCD. L1: cylindrical concave lens ($f=-25.4$ mm), L2: cylindrical convex lens ($f=400$ mm), L3: cylindrical convex lens ($f=1000$ mm), M: mirror, BD: beam dump. (b) Radiance curve for the calibration lamp as a function of wavelength. The blue and red regions depict the detection wavelength for the current study using the filters on the splitter.

The image pairs acquired for a given test condition is first split to obtain intensities from the two different wavelengths separately to match the exact regions of interest on both the images. Since the pixelated intensities tend to give erroneous values when dividing the pixel values from the two image pairs, the images are smoothed using a 3×3 convolution filter. After applying the flat-field correction and removing any background noise, the soot temperature values are obtained using the Planck's law for blackbody radiation. The ratio of soot absorption function ($E(m)$) values at two different wavelengths is taken as 1.0. For the low-fluence LII regime, soot temperature values should not exceed the sublimation temperature, which is usually considered to be around 4000 K. The averaged soot temperature distribution for the case of Jet A fuel at the global equivalence ratio (ϕ_g) of 0.2 with 35.3 psig pressure and 450 K preheat is shown in Figure 9a. The temperature values lie below 4000K in the entire region, satisfying the low-fluence LII criterion. Although a laser sheet with uniform fluence should heat up the soot particles uniformly to the same temperature instantaneously, the differences in soot temperatures spatially can be due to several factors. The soot maturity will not be uniform throughout the flame and hence nascent soot and mature soot will heat up differently. Additionally, the laser fluence along the sheet is not completely top-hat; the fluence drops slightly towards the upstream direction. Nonetheless, the soot volume fraction is not affected by the differences in temperature as the current study uses the two-color ratiometric method in the low-fluence regime.

Once the soot temperature is obtained at all locations, the raw LII signals can be quantified using the radiance values from the calibration lamp at the same camera settings. The mean soot volume fractions (f_v) for the Jet A fuel case at $\phi_g=0.2$ is shown in Figure 9b. The masked regions in images are due to the quench holes of the combustor inadvertently appearing in one of the image pairs which could not be avoided in the present measurements. The mean f_v values are below 5 ppm at most of the locations throughout the flame regions. The maximum values occur near the shear region of the conical spray where the main reactions occur as expected. The high values near the borders of the flame are due to insufficient signals over time leading to a higher mean. So, the actual time-averaged values should be lower than the values depicted in Figure 9b. Due to the highly turbulent nature of the flame along with the swirling nature of the flow, the soot detection probabilities are much lower than a laminar flame case at a given location. Hence, 500 images may not be sufficient for obtaining a converged soot volume fraction distribution for a given condition. Another important feature to notice in the contours is that the laser extinction along the beam path from right to left in Figure 9b can also make the f_v values to appear to be decreasing for the same regions downstream of the different fuel injectors. This absorption will be hard to correct as the soot concentration and their extinction coefficients must be known instantaneously throughout the flame

region. Improvements to most of these measurement features will be made in future campaigns to obtain more accurate soot distributions.

To study the effect of the type of fuel, the same LII measurements were made with SAF as the fuel at similar conditions to Jet A fuel. Since SAF has different fuel physical and chemical properties, the soot formation tendencies are expected to differ.

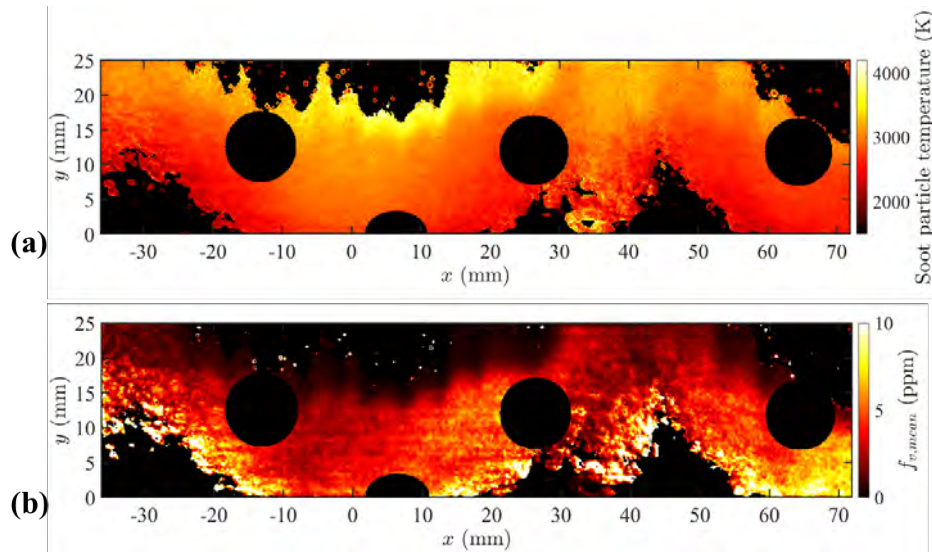


Figure 9. Spatial mean contours of (a) soot particle temperature and (b) soot volume fraction for Jet A combustion at 35.3 psig pressure, 450 K preheat and global equivalence ratio of 0.2. The black masked regions are from the quench holes appearing in the images.

The f_v contours for both Jet A fuel and SAF are shown in Figure 10 for the same operating conditions and global equivalence ratio. There is a considerable difference seen in the soot volume fraction values for the case of SAF as compared to Jet A fuel. The f_v values are almost 2-3 times lower for SAF at the same spatial locations as the Jet A fuel case. This is mainly due to the chemical composition of SAF utilized in the current study. As there is a negligible number of aromatics present in SAF, the tendencies for soot precursor formation is reduced leading to reduced overall soot production. Comparing the spray properties in the previous section, SAF also produced slightly smaller droplets as compared to Jet A fuel which will contribute to better fuel-air mixing and more complete combustion. Although the contribution from differences in spray is much lower as compared to the contribution from the chemical effects, the combined effects help in reducing soot formation considerably in the case of SAF combustion. Further processing of LII results is underway at more operating conditions for both Jet A fuel and SAF which will provide a comprehensive understanding of soot formation properties of these fuels at different conditions. These results will be reported in the next year's annual report.

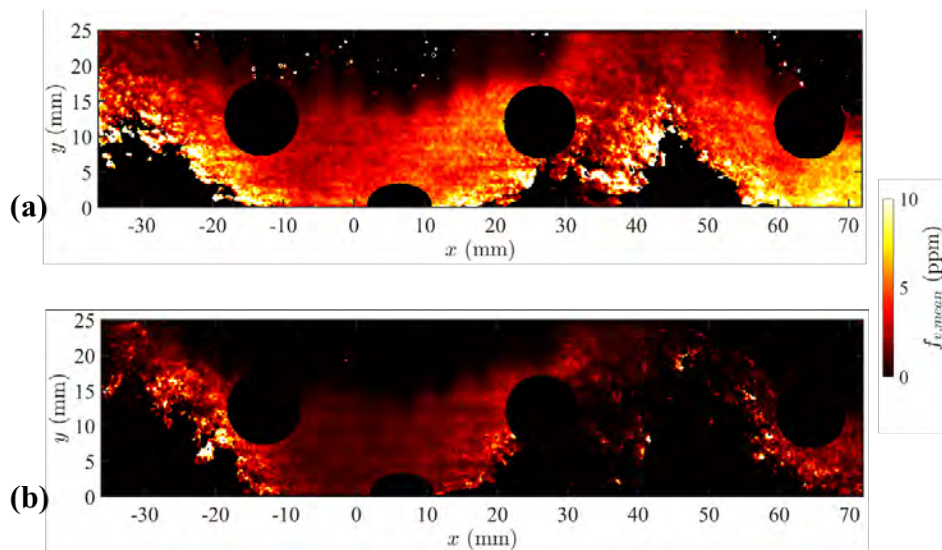


Figure 10. Spatial mean contours of soot volume fraction for (a) Jet A fuel and (b) SAF reacting flow at 35.3 psig pressure, 450 K preheat and global equivalence ratio of 0.2. The black masked regions are from the quench holes appearing in the images.

Milestone

- Conducted systematic PDPA and two-color LII measurements at different combustor operating conditions with Jet A fuel, SAF, and a 50-50 blend of Jet A fuel and SAF, respectively.

Major Accomplishments

- Conducted spatially resolved droplet size measurements in a confined sector combustor using PDPA for Jet A fuel, SAF, and a 50-50 blend of Jet A fuel and SAF.
- Conducted two-color LII measurements to obtain nvPM volume fraction distributions at different combustor operating conditions for Jet A and SAF.
- Compared the differences between Jet A and SAF in terms of spray properties and nvPM formation.

Publications

McGrath, R., Juergensmeyer, J., Bond, R., Bugay, E., Wehe, S., Wu, D., Steinberg, A., Sun, W., & Mazumdar, Y. C. (2024). Planar laser-induced incandescence for the study of soot production in a multi-sector RQL Jet A combustor. *Applications in Energy and Combustion Science*, 18, 100269.

<https://doi.org/10.1016/j.jaecs.2024.100269>

Vishwanath, R., Bibik, O., Olimid, D., Douglas, E., Wehe, S., Mazumdar, Y. C., Steinberg, A., & Sun, W. (2025, January 12-16). *Drop-size measurements using phase doppler particle anemometry in a confined high-pressure sector combustor* [Conference presentation]. AIAA SciTech 2025 Forum, Orlando, Florida.

Juergensmeyer, J., Miller, J., Bond, R., McGrath, R., Wehe, S., Sun, W., Mazumdar, Y. C., & Steinberg, A. (2025, June 16-20). Measurement of particulate matter and its oxidation in a multi-sector rich-quench-lean combustor. ASME Turbomachinery Technical Conference & Exposition 2025, Memphis, Tennessee.

Outreach Efforts

None.

Awards

Dr. Wenting Sun received the Hiroshi Tsuji Early Career Researcher Award (2023). This award is awarded by the Combustion Institute, which recognizes early career researchers who have demonstrated excellence in fundamental or applied combustion science and have achieved a significant advancement in their field within four to ten years of

completing a doctoral degree or equivalents. Dr. Wenting Sun was made an American Institute of Aeronautics and Astronautics (AIAA) Associated Fellow in 2023.

Dr. Adam Steinberg was made a fellow of The Combustion Institute in 2023.

Student Involvement

Four graduate students, Adhav Arulanandan, Dominic Olimid, Eric Douglas, and Andrew Fan, from Georgia Tech worked on Task 1.

Plans for Next Period

- Conduct PDPA, two-color LII, and OH radical planar laser induced fluorescence (OH PLIF) measurements in a new combustor configuration for Jet A fuel, SAF, and their blends at a large range of operating conditions.
- Continue detailed combustor design and comprehensive thermal stress analysis.